

The effect of heterovalent $P^{+5} \leftrightarrow Si^{+4}$ substitution on the microhardness of $Ag_{7+x}(P_{1-x}Si_x)S_6$ single crystals

I.O. Shender^{1*}, A.I. Pogodin^{1**}, M.J. Filep^{1,2}, T.O. Malakhovska¹, O.P. Kokhan¹, L.M. Suslikov¹, V.S. Bilanych¹, R. Mariychuk³

¹Uzhhorod National University, 46, Pidhirna str., 88000 Uzhhorod, Ukraine

²Ferenc Rákóczi II Transcarpathian Hungarian Institute, Kossuth Sq. 6, 90200 Beregovo, Ukraine

³University of Presov, 17th November 1, 08116 Presov, Slovakia

Corresponding authors e-mail: iryina.shender@uzhnu.edu.ua*, artempogodin88@gmail.com**

Abstract. Herein, we present the results of the microhardness investigations of $Ag_{7+x}(P_{1-x}Si_x)S_6$ ($x = 0, 0.1, 0.25, 0.5, 0.75, 1$) single crystals. The influence of composition x on the dependence of microhardness on the applied load was investigated. The study was carried out within a wide range of the applied loads 0.05...2 N. It has been found that an increase in the load on the indenter leads to a monotonic nonlinear decrease in the values of microhardness in all studied samples. This indicates a “normal” indentation size effect. The observed effect in $Ag_{7+x}(P_{1-x}Si_x)S_6$ single crystals at various x was described using the geometrically necessary dislocations model. The corresponding parameters of the geometrically necessary dislocations model were determined. The influence of ionic radii and electronegativity of structural polyhedra elements of $Ag_{7+x}(P_{1-x}Si_x)S_6$ solid solutions was discussed.

Keywords: argyrodite, single crystal, microhardness, heterovalent substitution.

<https://doi.org/10.15407/spqeo28.01.026>

PACS 62.20.Qp, 66.30.H-, 81.10.Fq

Manuscript received 28.11.24; revised version received 31.01.25; accepted for publication 12.03.25; published online 26.03.25.

1. Introduction

Superionic conductors are promising materials showing an unusually high ionic conductivity in the solid state, which makes them useful in scientific and technological fields. Their high ionic conductivity creates prospects for developing efficient energy systems, namely solid-state batteries and fuel cells, where the speed and effectivity of ion transport are crucial factors [1–4]. Superionic conductors contribute to improving electrolysis and catalysis methods, offering new opportunities to increase the efficiency of chemical reactions. Due to their significant potential for optimization and innovation, these materials continue to attract the attention of researchers and engineers in various fields, opening up new horizons for process improvement [5–7].

Today, the ability of materials to withstand various mechanical loads is an important factor in ensuring their performance characteristics, namely durability and stability, and optimizing their composition can increase the strength of materials, which is critical for applications in the latest technologies. To accurately determine the mechanical properties of materials, the microhardness measurements are used. This method allows us to assess

the materials resistance to local deformation and surface damage at the micro level. Microhardness measurements give researchers detailed data on how a material behaves under load, which helps to tune its properties to achieve optimum strength and wear resistance. This is important for developing high-performance materials used in solid-state batteries and microelectronic components, as high microhardness prevents mechanical damage and deformation due to external factors [8–13].

The microhardness of superionic conductors allows estimating their strength and mechanical stability, which is important for highly conductive materials. Microhardness tests can provide insight into local mechanical properties, particularly in the presence of a heterogeneous structure or defects in material. Microhardness testing also provides an opportunity to perform a comparative analysis of different materials and estimate the impact of crystal structure on mechanical properties. Superionic conductors can exhibit different microhardness depending on their composition and structural features. The Vickers method, based on the application of tetrahedral pyramidal indenter, allows measuring microhardness even in small single-crystal samples, which is important from a practical point of view for experimental studies.

Despite the large number of superionic phases, the study of their mechanical properties is limited to only a few classes of lithium-containing compounds. Most of the works report on the study of oxide superionic materials such as garnet ($\text{Li}_7\text{La}_3\text{Zr}_2\text{O}_{12}$) and perovskite ($\text{Li}_{0.35}\text{La}_{0.557}\text{TiO}_3$) types obtained in the form of ceramics, and LIPON-type ($\text{Li}_x\text{PO}_y\text{N}_z$) samples in form of amorphous glass thin films. The garnet and perovskite phases have a significant hardness in the range of 4.7 to 18 GPa [14, 15], meanwhile LIPONs have lower hardness 1.5...5.8 GPa [15]. Microhardness of sulfide based solid electrolytes was studied for different compositions of $\text{Li}_2\text{S-P}_2\text{S}_5$ system in form of amorphous glass and is about 1.9 GPa [15]. Studies of superionic materials in the single crystal ($\text{Ag}_7(\text{Si}_{1-x}\text{Ge}_x)\text{S}_5\text{I}$, $\text{Ag}_{6+x}(\text{P}_{1-x}\text{Ge}_x)\text{S}_5\text{I}$) form are limited to the results reported by us earlier [13, 16–18]. The microhardness of these phases is in range 0.90...1.15 GPa.

This work aims to investigate the behavior of microhardness of $\text{Ag}_{7+x}(\text{P}_{1-x}\text{Si}_x)\text{S}_6$ superionic crystals at various compositions x and describe it using the geometrically necessary dislocations model (Nix–Gao model).

2. Experimental

The synthesis of $\text{Ag}_{7+x}(\text{P}_{1-x}\text{Si}_x)\text{S}_6$ solid solutions with the composition $x = 0.1, 0.25, 0.5, \text{ and } 0.75$ was carried out using the one-temperature synthesis method in evacuated to 0.13 Pa quartz ampoules from previously synthesized Ag_7PS_6 and Ag_8SiS_6 [19] taken in corresponding molar ratios. The process of synthesis of ternary chalcogenides Ag_7PS_6 and Ag_8SiS_6 is described in detail in previous studies [19, 20]. The maximum synthesis temperature at which all $\text{Ag}_{7+x}(\text{P}_{1-x}\text{Si}_x)\text{S}_6$ compositions were in the molten state was 1015 °C, and all alloys were kept at this temperature for 72 h [19]. After that, all $\text{Ag}_{7+x}(\text{P}_{1-x}\text{Si}_x)\text{S}_6$

compositions were cooled to room temperature at a rate of 50 °C/h. As a result, bulk polycrystalline alloys $\text{Ag}_{7+x}(\text{P}_{1-x}\text{Si}_x)\text{S}_6$ with $x = 0, 0.1, 0.25, 0.5, 0.75, \text{ and } 1$ with weight of 22 g each sample were obtained, and the corresponding single crystals were subsequently grown from the melt by the directed crystallization method [19]. The single crystals were grown in conical evacuated quartz ampoules according to the procedure described in Ref. [19]. As a result, single crystals of dark grey color with a metallic luster, 4 cm long and 1.2 cm in diameter were obtained [19].

The microhardness of $\text{Ag}_{7+x}(\text{P}_{1-x}\text{Si}_x)\text{S}_6$ single crystals was studied at room temperature by using a PMT-3 tester equipped with a Vickers diamond indenter (a regular quadrangular pyramid with an angle at the vertex of 136°). Before the experimental studies, the cut-off samples were polished by abrasive powders and diamond abrasive pastes to optical quality.

It should be noted that the load on the indenter was within the range of 0.05 to 2 N and the indentation time at each constant load was 10 s. The diagonal lengths of each resulting Vickers indentation were measured using an attached optical microscope. Six indentations were made at each load, while the distance between two indentations was at least three times the resulting diagonal length. It is worth noting that at the maximum load on the indenter, the maximum depth of the imprint was within 7.5...8.5 μm, depending on the composition x .

The load-dependent Vickers microhardness (H) was estimated using the known relation [21]:

$$H = \frac{2P \sin(\alpha/2)}{d^2} = 1.854 \frac{P}{d^2}, \quad (1)$$

where α is the angle of the Vickers vertex, P – load applied on the indenter, and d – diagonal of the imprint.

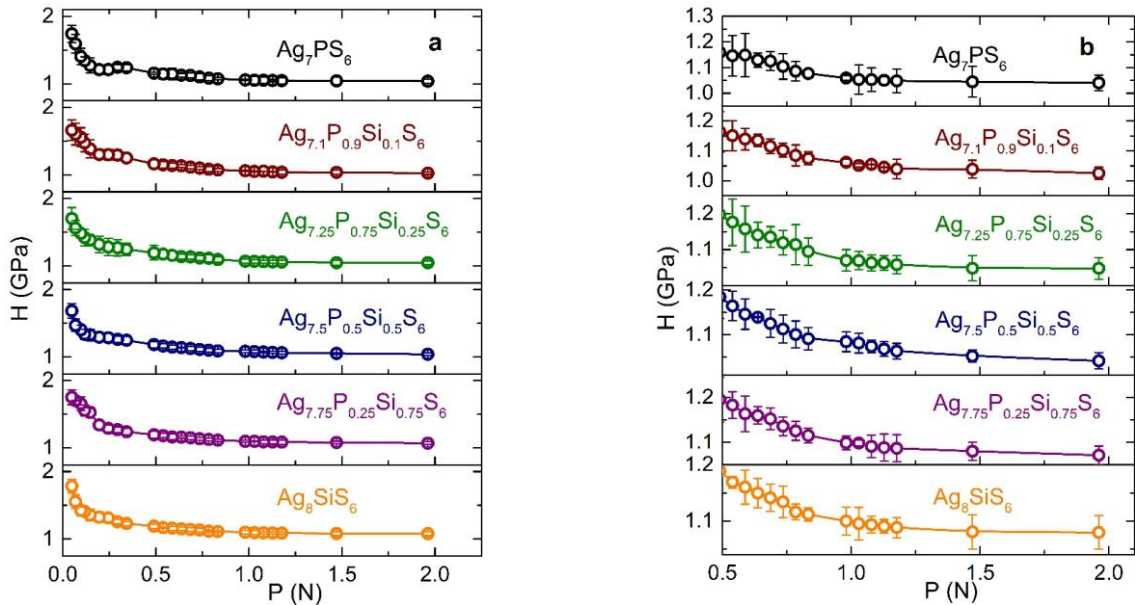


Fig. 1. Dependences of the microhardness H on the indenter load P for $\text{Ag}_{7+x}(\text{P}_{1-x}\text{Si}_x)\text{S}_6$ single crystals: overall view of the curve (a) and detailed in the region of higher loads (b).

3. Results and discussion

The results of our studies have shown that for the crystals of individual ternary chalcogenides Ag_7PS_6 , Ag_8SiS_6 as well as for the solid solutions $\text{Ag}_{7.1}\text{P}_{0.9}\text{Si}_{0.1}\text{S}_6$, $\text{Ag}_{7.25}\text{P}_{0.75}\text{Si}_{0.25}\text{S}_6$, $\text{Ag}_{7.5}\text{P}_{0.5}\text{Si}_{0.5}\text{S}_6$, and $\text{Ag}_{7.75}\text{P}_{0.25}\text{Si}_{0.75}\text{S}_6$ an increase in the load on the indenter P leads to the monotonic nonlinear decrease in the values of microhardness H (Fig. 1).

One can see that an increase in the load on the indenter P within 0.05...0.3 N leads to a sharp decrease in the microhardness, while a further increase in the load leads to the unsubstantial decrease in the microhardness indicating a “normal” indentation size effect (ISE) in the studied crystals [22, 23].

It is worth noting that the formation of the imprint at the low loads (within the range $\sim 0.05\dots 0.3$ N) occurs mainly due to the plastic deformation of single crystals under the indenter, while at higher loads, it is due to the compaction of single crystals [24–26].

Fig. 2 shows that, regardless of the applied load, the microhardness increases monotonically with the x value. Thus, at 1.5 N load the increase is $\Delta H = 0.04$ GPa, from 1.04 GPa for $x = 0$ to 1.08 GPa for $x = 1$. The tendency of microhardness values to grow is associated with different electronegativities of P, Si and S elements ($\chi(\text{P}) = 2.19$, $\chi(\text{Si}) = 1.90$ and $\chi(\text{S}) = 2.58$ [27]), which form the basic structural polyhedral ($[\text{PS}_4]$, $[\text{SiS}_4]$, $[(\text{PSi})\text{S}_4]$) of the anionic sublattices in individual chalcogenides Ag_7PS_6 , Ag_8SiS_6 and solid solutions $\text{Ag}_{7+x}(\text{P}_{1-x}\text{Si}_x)\text{S}_6$ [19]. The observed electronegativity difference in ternary compounds is $|\Delta\chi(\text{P-S})| = 0.39$, $|\Delta\chi(\text{Si-S})| = 0.68$, and gradually changes in solid solutions. Electronegativity difference growth leads to an increase in bond rigidity and, consequently, a decrease in the compressibility of coordination polyhedra. A similar microhardness behavior was observed earlier when we studied the change in microhardness in the crystals $\text{Ag}_{6+x}(\text{P}_{1-x}\text{Ge}_x)\text{S}_5\text{I}$, $\text{Ag}_{7+x}(\text{P}_{1-x}\text{Ge}_x)\text{S}_6$, $\text{Ag}_7(\text{Si}_{1-x}\text{Ge}_x)\text{S}_5\text{I}$ formed by heterovalent $\text{P}^{+5} \rightarrow \text{Ge}^{+4}$ and isovalent $\text{Si}^{+4} \rightarrow \text{Ge}^{+4}$ substitutions [16–18]. Thus, for systems $\text{Ag}_{6+x}(\text{P}_{1-x}\text{Ge}_x)\text{S}_5\text{I}$, $\text{Ag}_{7+x}(\text{P}_{1-x}\text{Ge}_x)\text{S}_6$, the increase in electronegativity difference ($|\Delta\chi(\text{P-S})| = 0.39$, $|\Delta\chi(\text{Si-S})| = 0.68$) causes a microhardness values growth, meanwhile in the case of $\text{Ag}_7(\text{Si}_{1-x}\text{Ge}_x)\text{S}_5\text{I}$ the decreasing in electronegativity difference ($|\Delta\chi(\text{Si-S})| = 0.68$, $|\Delta\chi(\text{Ge-S})| = 0.57$) and microhardness is observed. Namely, the microhardness difference in $\text{Ag}_{6+x}(\text{P}_{1-x}\text{Ge}_x)\text{S}_5\text{I}$ system equals 0.15 GPa [16], for $\text{Ag}_{7+x}(\text{P}_{1-x}\text{Ge}_x)\text{S}_6$ is 0.11 GPa [17], and for $\text{Ag}_7(\text{Si}_{1-x}\text{Ge}_x)\text{S}_5\text{I}$ is 0.06 GPa [18] at 1.5 N.

As can be seen from Refs [16–18], cationic substitution ($\text{P}^{+5} \rightarrow \text{Ge}^{+4}$ and $\text{Si}^{+4} \rightarrow \text{Ge}^{+4}$) led to larger changes in microhardness values, which is obviously related to the larger differences ($|\Delta R_I(\text{P}^{+5}-\text{Ge}^{+4})| = 0.015$ nm; $|\Delta R_I(\text{Si}^{+4}-\text{Ge}^{+4})| = 0.013$ nm) between their ionic radii ($R_I(\text{P}^{+5}) = 0.038$ nm; $R_I(\text{Ge}^{+4}) = 0.053$ nm; $R_I(\text{Si}^{+4}) = 0.040$ nm) [28]. Thus, a slight increase in microhardness (Fig. 2) was associated with the closeness of the ionic radii of P^{+5} and Si^{+4} [28], the difference between which is only $|\Delta R_I(\text{P}^{+5}-\text{Si}^{+4})| = 0.002$ nm, which leads to a very slight increase in the rigidity of the crystal structure.

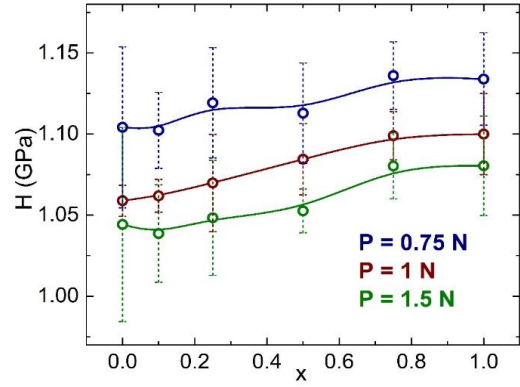


Fig. 2. Compositional dependence of the microhardness of $\text{Ag}_{7+x}(\text{P}_{1-x}\text{Si}_x)\text{S}_6$ single crystals at different indenter loads.

Let us consider in detail the effect of heterovalent cationic $\text{P}^{+5} \rightarrow \text{Si}^{+4}$ substitution on the change in the microhardness of $\text{Ag}_{7+x}(\text{P}_{1-x}\text{Si}_x)\text{S}_6$ single crystals within the framework of the gradient theory of plasticity. The appearance of size effect, during the indentation process, indicates a greater number and activity of dislocations in the material. Nix and Gao explained the ISE by introducing the concept of geometrically necessary dislocations (GND) formed during the indentation process to distinguish them from the existing statistically distributed dislocations using the following equation [29, 30]:

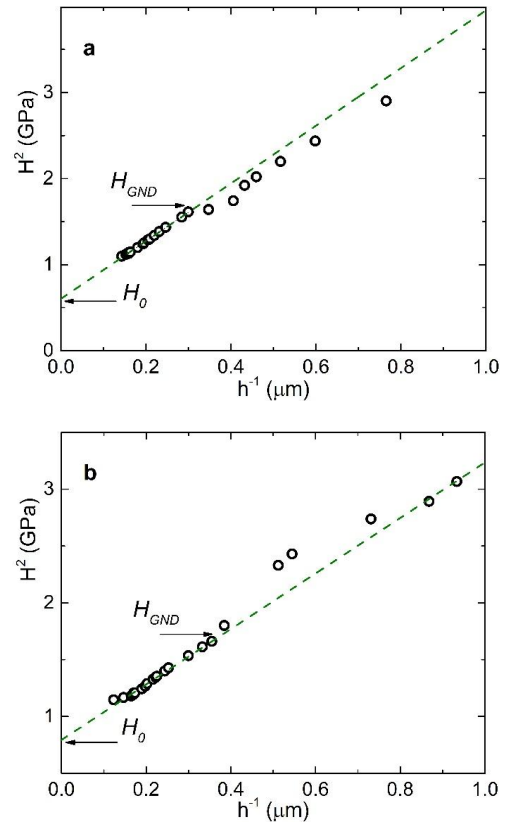


Fig. 3. The Nix–Gao plot H^2 vs h^{-1} of $\text{Ag}_{7.25}\text{P}_{0.75}\text{Si}_{0.25}\text{S}_6$ (a) and $\text{Ag}_{7.75}\text{P}_{0.25}\text{Si}_{0.75}\text{S}_6$ (b) single crystals (black circles – experimental data, dashed line – approximated microhardness).

Table. Parameters of the GND model for $\text{Ag}_{7+x}(\text{P}_{1-x}\text{Si}_x)\text{S}_6$ single crystals.

| Composition | h^* , μm | H_0 , GPa | h_{GND} , μm | H_{GND} , GPa |
|---|-----------------------|-------------|----------------------------------|------------------------|
| Ag_7PS_6 | 0.214 | 0.797 | 4.08 | 1.17 |
| $\text{Ag}_{7.1}\text{P}_{0.9}\text{Si}_{0.1}\text{S}_6$ | 0.182 | 0.769 | 3.05 | 1.27 |
| $\text{Ag}_{7.25}\text{P}_{0.75}\text{Si}_{0.25}\text{S}_6$ | 0.180 | 0.777 | 3.34 | 1.27 |
| $\text{Ag}_{7.5}\text{P}_{0.5}\text{Si}_{0.5}\text{S}_6$ | 0.241 | 0.829 | 3.12 | 1.26 |
| $\text{Ag}_{7.75}\text{P}_{0.25}\text{Si}_{0.75}\text{S}_6$ | 0.307 | 0.881 | 2.82 | 1.28 |
| Ag_8SiS_6 | 0.276 | 0.879 | 3.35 | 1.26 |

$$\frac{H}{H_0} = \sqrt{1 + \frac{h^*}{h}}, \quad (2)$$

where H and h are the measured microhardness and indentation depth, respectively. H_0 is the hardness that would arise from the statistically stored dislocations alone, in the absence of any geometrically necessary dislocations, and h^* is a correlation dimension, related to indenter geometry, elastic shear modulus, and hardening property.

To ascertain the parameters of the Nix–Gao model, the linear form of Eq. (2) was used:

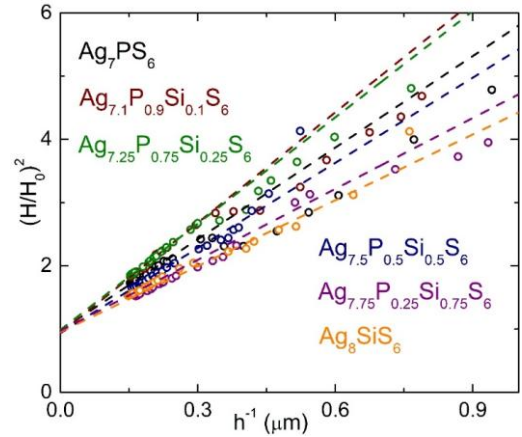
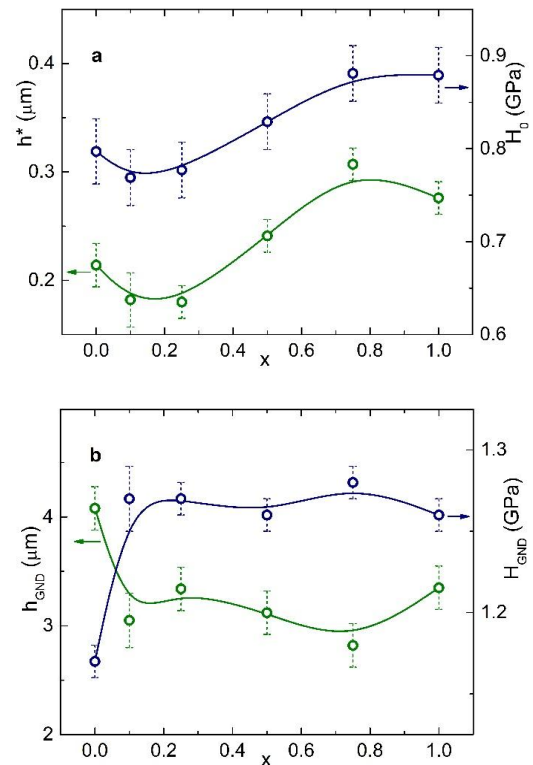
$$H^2 = H_0^2 + (H_0^2 \cdot h^*) \cdot h^{-1}. \quad (3)$$

According to this approximation, the parameter H_0 , which is the hardness considering intrinsic dislocations, is determined as the point of intersection of the line with the ordinate axis. The value of the correlation size h^* was determined based on the angle tangent of the line to the abscissa axis, taking into account H_0 . The values of H_{GND} and h_{GND} can be determined from the graphical dependence at the beginning of deviation from the straight line.

Thus, the dependence H^2 vs h^{-1} was constructed for all compositions of $\text{Ag}_{7+x}(\text{P}_{1-x}\text{Si}_x)\text{S}_6$ crystals. As it seen from Fig. 3 for all studied compositions, the presence of a linear region (Fig. 3) of the H^2 vs h^{-1} dependence was obtained. The linear dependence of H^2 on the imprint depth h^{-1} indicates the presence of plastic deformation in the studied single crystals. This made it possible to ascertain the parameters of the GND model (Table).

Here, H_{GND} is the microhardness of the crystal at which the contribution of geometrically necessary dislocations begins to appear in plastic deformation during indentation process. h_{GND} is the minimum depth of the indenter imprint, which is sufficient for formation of geometrically necessary dislocations [29].

To confirm the correctness of application of the GND model and determined parameters of the model, the $(H/H_0)^2$ on h^{-1} dependences were constructed. As it seen from Fig. 4, all extrapolated data at $h \rightarrow \infty$ intersect in one point with value 1. This implies if $h \rightarrow \infty$, then $H \rightarrow H_0$. It was found that for all $\text{Ag}_{7+x}(\text{P}_{1-x}\text{Si}_x)\text{S}_6$ single crystals this condition is fulfilled (Fig. 4), which once again confirms the application of this model. Finally, we consider the effect of heterovalent cationic $\text{P}^{+5} \rightarrow \text{Si}^{+4}$ substitution on the change in the parameters of the GND model: h^* , H_0 , h_{GND} , and H_{GND} (Fig. 5) for all compositions x .


Fig. 4. Dependences of $(H/H_0)^2$ on h^{-1} for all studied compositions x of $\text{Ag}_{7+x}(\text{P}_{1-x}\text{Si}_x)\text{S}_6$ crystals. (Color online)

Fig. 5. Compositional dependence of the GND model parameters: h^* , H_0 (a) and h_{GND} , H_{GND} (b) for the $\text{Ag}_{7+x}(\text{P}_{1-x}\text{Si}_x)\text{S}_6$ single crystals.

It has been found that heterovalent cationic $P^{+5} \rightarrow Si^{+4}$ substitution in single crystals of $Ag_{7+x}(P_{1-x}Si_x)S_6$ solid solutions leads to a nonlinear non-monotonic increase in the parameters h^* (correlation size) and H_0 (Fig. 5a). These are demonstrated in the presence of a minimum for solid solutions with $x = 0.1$ and $x = 0.25$ and a slight maximum observed for the solid solution of the $x = 0.75$ composition (Fig. 5a), as compared to the initial ternary chalcogenides Ag_7PS_6 and Ag_8SiS_6 , with these extreme points being more pronounced for the h^* parameter than for H_0 . It should be noted that this behavior of the h^* parameter indicates that the highest density of statistically distributed dislocations is observed in the $x = 0.1$, and $x = 0.25$ single crystals, and the lowest in the $x = 0.25$ single crystal. If we consider the change (Fig. 5a) of the parameter H_0 , or the value of the ultimate microhardness, *i.e.*, the microhardness of the material without taking into account the additional effects caused by geometrically necessary dislocations, it becomes obvious that the compositional behavior of this parameter is quite similar to the compositional behavior of the microhardness (Fig. 2). The presence of a slight minimum and maximum in the compositional dependence of the ultimate microhardness (Fig. 5a) is most likely caused by the disorder of the crystal structure (anionic sublattice) caused by the heterovalent cationic $P^{+5} \rightarrow Si^{+4}$ substitution [14]. The non-monotonic nonlinear behavior of the h_{GND} and H_{GND} parameters (Fig. 5b), which is demonstrated in the presence of a minimum for the h_{GND} parameter and, accordingly, a maximum for the H_{GND} parameter for $Ag_{7+x}(P_{1-x}Si_x)S_6$ with $x = 0.1$, 0.25 , 0.5 , 0.75 solid solutions in comparison with initial Ag_7PS_6 and Ag_8SiS_6 , is most likely related to the peculiarities of solid solutions formation. Namely, due to presence of heterovalent cationic $P^{+5} \rightarrow Si^{+4}$ substitution, of atom with different ionic radii and electronegativity, the disordering of cationic sublattice appears [19]. The ternary chalcogenides Ag_7PS_6 and Ag_8SiS_6 are characterized by a fairly ordered crystal structure, since the site occupancy factor of all symmetrically independent Ag positions is 1 [19, 20]. In the process of $Ag_{7+x}(P_{1-x}Si_x)S_6$ solid solutions formation, the anionic and, consequently, the cationic sublattices are disordered, *i.e.*, the site occupancy factor of Ag positions becomes less than 1 [19].

4. Conclusions

The microhardness of single crystals of $Ag_{7+x}(P_{1-x}Si_x)S_6$ ($x = 0, 0.1, 0.25, 0.5, 0.75, 1$) solid solutions was studied using the Vickers method. The dependence of the microhardness of single crystals of $Ag_{7+x}(P_{1-x}Si_x)S_6$ solid solutions on the depth of the imprint was interpreted within the framework of the geometrically necessary dislocations model (Nix and Gao theory) and the parameters of this model were determined. It was ascertained that for $Ag_{7+x}(P_{1-x}Si_x)S_6$ single crystals, $P^{+5} \rightarrow Si^{+4}$ substitution leads to a nonlinear variations of the parameters of Nix–Gao model. Thus, for h^* , H_0 and H_{GND} a nonlinear increasing, meanwhile for h_{GND} – nonlinear decreasing is observed.

It was found that with an increase in the ionic radius (R_I) of phosphorus and silicon at their heterovalent substitution, the rigidity of the crystal structure of the studied materials decreases. Thus, as a result of the disordered crystal structure, GNDs in $Ag_{7+x}(P_{1-x}Si_x)S_6$ solid solutions will occur at lower indenter loads, *i.e.*, at a lower imprint depth, which will lead to the fact that the effect of GNDs on the microhardness of single crystals will be manifested at higher microhardness values.

Acknowledgements

This work was supported by the grants of the National Scholarship Programme of the Slovak Republic [GrantID: 52200 and Grant ID: 52201].

The authors also thank the Armed Forces of Ukraine for providing security to perform this work. This work has become possible only because of the resilience and courage of the Ukrainian Army.

References

1. Laqibi M., Cros B., Peytavin S., Ribes M. New silver superionic conductors Ag_7XY_2Z ($X = Si, Ge, Sn; Y = S, Se; Z = Cl, Br, I$)-synthesis and electrical studies. *Solid State Ionics*. 1987. **23**. P. 21–26. [https://doi.org/10.1016/0167-2738\(87\)90077-4](https://doi.org/10.1016/0167-2738(87)90077-4).
2. Yugami H., Ishigame M. Fundamental physics and promising applications of superionic conductors. *Jpn. J. Appl. Phys.* 1993. **32**, No 2. P. 853–859. <https://doi.org/10.1143/jjap.32.853>.
3. Zhang Z., Shao Y., Lotsch B. *et al.* New horizons for inorganic solid state ion conductors. *Energy Environ. Sci.* 2018. **11**. P. 1945–1976. <https://doi.org/10.1039/C8EE01053F>.
4. Romaka V.V., Romaka V.A., Stadnyk Y.V. *et al.* Features of mechanisms of electrical conductivity in semiconductive solid solution $Lu_{1-x}Sc_xNiSb$. *Ukr. J. Phys.* 2022. **67**. P. 370–379. <https://doi.org/10.15407/ujpe67.5.370>.
5. Chen Y., Wen K., Chen T. *et al.* Recent progress in all-solid-state lithium batteries: The emerging strategies for advanced electrolytes and their interfaces. *Energy Storage Mater.* 2020. **31**. P. 401–433. <https://doi.org/10.1016/j.ensm.2020.05.019>.
6. Balkanski M. Applications of Superionic Conductors in Microbatteries and Elsewhere. In: *Atomic Diffusion in Disordered Materials: Theory and Applications*. Eds. Balkanski M., Elliott R. World Scientific, 1998. P. 239–295. https://doi.org/10.1142/9789812817327_0006.
7. Zhang Z., Zhang L., Liu Y. *et al.* Synthesis and characterization of argyrodite solid electrolytes for all-solid-state Li-ion batteries. *J. Alloys Compd.* 2018. **747**. P. 227–235. <https://doi.org/10.1016/j.jallcom.2018.03.027>.
8. Cheng E.J., Yang T., Liu Y. *et al.* Correlation between mechanical properties and ionic conductivity of sodium superionic conductors: a relative density-dependent relationship. *Materials Today Energy*. 2024. **44**. P. 101644. <https://doi.org/10.1016/j.mtener.2024.101644>.

9. Yan G., Yu S., Nonemacher J.F. *et al.* Influence of sintering temperature on conductivity and mechanical behavior of the solid electrolyte LTP. *Ceram. Int.* 2019. **45**, No 12. P. 14697–14703. <https://doi.org/10.1016/j.ceramint.2019.04.191>.
10. Zong Z., Lou J., Adewoye O.O. *et al.* Indentation size effects in the nano and microhardness of FCC single crystal metals. *Mater. Manuf. Process.* 2007. **22**, No 2. P. 228–237. <https://doi.org/10.1080/10426910601063410>.
11. Microelectromechanical Structures for Materials Research. Eds. Brown S., Gilbert J., Guckel H. *et al. Mater. Res. Soc. Proc.* 1998. **518**.
12. Nonemacher J.F., Naqash S., Tietz F., Malzbender J. Micromechanical assessment of Al/Y-substituted NASICON solid electrolytes. *Ceram. Int.* 2019. **45**, No 17, Part A. P. 21308–21314. <https://doi.org/10.1016/j.ceramint.2019.07.114>.
13. Pogodin A.I., Filep M.J., Malakhovska T.O. *et al.* Microstructural, mechanical and electrical properties of superionic $\text{Ag}_{6+x}(\text{P}_{1-x}\text{Ge}_x)\text{S}_5\text{I}$ ceramic materials. *J. Phys. Chem. Sol.* 2022. **171**. P. 111042. <https://doi.org/10.1016/j.jpcs.2022.111042>.
14. Wang A.N., Nonemacher J.F., Yan G. *et al.* Mechanical properties of the solid electrolyte Al-substituted $\text{Li}_7\text{La}_3\text{Zr}_2\text{O}_{12}$ (LLZO) by utilizing micro-pillar indentation splitting test. *J. Eur. Ceram. Soc.* 2018. **38**. P. 3201–3209. <https://doi.org/10.1016/j.jeurceramsoc.2018.02.032>.
15. Ke X., Wang Y., Ren G., Yuan C. Towards rational mechanical design of inorganic solid electrolytes for all-solid-state lithium ion batteries. *Energy Storage Mater.* 2020. **26**. P. 313–324. <https://doi.org/10.1016/j.ensm.2019.08.029>.
16. Shender I., Pogodin A., Aleksyk V. *et al.* Mechanical properties of single crystals based on $\text{Ag}_{6+x}(\text{P}_{1-x}\text{Ge}_x)\text{S}_5\text{I}$ solid solutions. *2021 IEEE 12th Int. Conf. on Electronics and Information Technologies (ELIT)*, Lviv, Ukraine, 2021. P. 10–13. <https://doi.org/10.1109/ELIT53502.2021.9501088>.
17. Shender I.O., Pogodin A.I., Filep M.J. *et al.* Microhardness of single-crystal samples of $\text{Ag}_{7+x}(\text{P}_{1-x}\text{Ge}_x)\text{S}_6$ solid solutions. *SPQEO*. 2024. **27**. P. 169–175. <https://doi.org/10.15407/spqeo27.02.169>.
18. Shender I.O., Pogodin A.I., Filep M.J. *et al.* Influence of cation $\text{Si}^{4+} \leftrightarrow \text{Ge}^{4+}$ and $\text{P}^{5+} \leftrightarrow \text{Ge}^{4+}$ substitution on the mechanical parameters of single crystals $\text{Ag}_7(\text{Si}_{1-x}\text{Ge}_x)\text{S}_5\text{I}$ and $\text{Ag}_{6+x}(\text{P}_{1-x}\text{Ge}_x)\text{S}_5\text{I}$. *SPQEO*. 2023. **26**. P. 408–414. <https://doi.org/10.15407/spqeo26.04.408>.
19. Pogodin A., Filep M., Malakhovska T. *et al.* Obtaining of disordered highly ionic conductive $\text{Ag}_{7+x}(\text{P}_{1-x}\text{Si}_x)\text{S}_6$ single crystalline materials. *Mat. Res. Bull.* 2024. **179**. P. 112953. <https://doi.org/10.1016/j.materresbull.2024.112953>.
20. Pogodin A.I., Filep M.J., Izai V.Yu. *et al.* Crystal growth and electrical conductivity of Ag_7PS_6 and Ag_8GeS_6 argyrodites. *J. Phys. Chem. Sol.* 2022. **168**. P. 110828. <https://doi.org/10.1016/j.jpcs.2022.110828>.
21. Filho P.P., Mitchell M.R., Link R.E. *et al.* Brinell and Vickers hardness measurement using image processing and analysis techniques. *J. Test. Evaluation*. 2010. **38**, No 1. P. 102220. <https://doi.org/10.1520/jte102220>.
22. Nabarro F.R., Shrivastava S., Luyckx S.B. The size effect in microindentation. *Phil. Mag.* 2006. **86**, No 25–26. P. 4173–4180. <https://doi.org/10.1080/14786430600577910>.
23. Benet C.J., Gnanam F.D. Vickers micromechanical indentation of NaSb_2F_7 and $\text{Na}_3\text{Sb}_4\text{F}_{15}$ single crystals. 1990. **9**, No 2. P. 165–166. <https://doi.org/10.1007/bf00727704>.
24. Karaca I., Büyükakkas S. Microhardness characterization of Fe- and Co-based superalloys. *Iran. J. Sci. Technol. Trans. Sci.* 2019. **43**. P. 1311–1319. <https://doi.org/10.1007/s40995-018-0604-y>.
25. Güder H.S., Şahin E., Şahin O. *et al.* Vickers and Knoop indentation microhardness study of β -SiAlON ceramic. *Acta Phys. Pol. A*. 2011. **120**. P. 1026–1033. <https://doi.org/10.12693/APhysPolA.120.1026>.
26. Luo Q., Kitchen M. Microhardness, Indentation size effect and real hardness of plastically deformed austenitic hadfield steel. *Materials*. 2023. **16**. P. 1117. <https://doi.org/10.3390/ma16031117>.
27. Allen L.C. Electronegativity is the average one-electron energy of the valence-shell electrons in ground-state free atoms. *J. Am. Chem. Soc.* 1989. **111**, No 25. P. 9003–9014. <https://doi.org/10.1021/ja00207a003>.
28. Shannon R.D. Revised effective ionic radii and systematic studies of interatomic distances in halides and chalcogenides. *Acta Cryst. A*. 1976. **32**. P. 751–767. <https://doi.org/10.1107/S0567739476001551>.
29. Nix W.D., Gao H. Indentation size effects in crystalline materials: A law for strain gradient plasticity. *J. Mech. Phys. Solids*. 1998. **46**. P. 411–425. [https://doi.org/10.1016/S0022-5096\(97\)00086-0](https://doi.org/10.1016/S0022-5096(97)00086-0).
30. Song P., Yabuuchi K., Spaetig P. Insights into hardening, plastically deformed zone and geometrically necessary dislocations of two ion-irradiated FeCrAl(Zr)-ODS ferritic steels: A combined experimental and simulation study. *Acta Mater.* 2022. **234**. P. 117991. <https://doi.org/10.1016/j.actamat.2022.117991>.

Authors' contributions

Shender I.O.: investigation, writing – original draft.

Pogodin A.I.: conceptualization, investigation, supervision, writing – review & editing.

Filep M.J.: investigation, visualization, writing – review & editing.

Malakhovska T.O.: methodology, writing – review & editing.

Kokhan O.P.: investigation, writing – original draft.

Suslikov L.M.: methodology, investigation.

Bilanych V.S.: investigation, visualization.

Mariychuk R.: methodology, conceptualization.

Authors and CV



Iryna O. Shender, defended her PhD thesis at the Uzhhorod National University in 2024. Authored 32 scientific papers and 7 patents. The area of her scientific interests is electrical, optical and mechanical properties of superionic conductors.

<https://orcid.org/0000-0003-1687-3634>



Artem I. Pogodin, PhD, Senior Researcher at the Uzhhorod National University. Authored over 100 scientific papers and 114 patents. The area of his scientific interests includes solid state chemistry, crystal growth and materials science.

<https://orcid.org/0000-0002-2430-3220>



Mykhailo J. Filep, PhD, Senior Researcher at the Uzhhorod National University, Associate Professor at the Ferenc Rákóczi II Transcarpathian Hungarian Institute. Authored over 100 scientific papers and 50 patents. The area of his scientific interests

includes solid state chemistry and materials science.

E-mail: mfilep23@gmail.com,

<http://orcid.org/0000-0001-7017-5437>



Tetyana O. Malakhovska, PhD, Senior Researcher at the Uzhhorod National University. Authored 70 scientific papers and 10 patents. The area of her scientific interests includes solid state chemistry and materials science. E-mail:

t.malakhovska@gmail.com,

<https://orcid.org/0000-0001-7309-4894>



Oleksandr P. Kokhan, PhD, Associate Professor at the Uzhhorod National University. Authored over 80 scientific papers and 95 patents. The area of his scientific interests includes inorganic chemistry, solid state chemistry, crystal growth, and

materials science. E-mail: aleksandr.kokh@gmail.com,
<http://orcid.org/0000-0003-1534-6779>



Leonid M. Suslikov, Doctor of Sciences, Professor at the Uzhhorod National University. Authored over 200 articles, 22 patents, 2 monographs, 42 textbooks. The area of scientific interests includes solid state physics, optical properties of complex semiconductor compounds.

E-mail: leonus48@gmail.com,

<https://orcid.org/0000-0003-4628-5972>



Vitaliy S. Bilanych, PhD, Associate Professor at the Uzhhorod National University. Authored over 80 publications. The area of his scientific interests includes physical properties of non-crystalline semiconductors and relaxation phenomena in chalcogenide

materials. E-mail: vbilanych@gmail.com,

<https://orcid.org/0000-0003-4293-5675>



Ruslan Mariychuk, PhD, Associate Professor at the University of Presov, Slovakia. Author of over 60 publications and 3 patents. His research interests include green chemistry, sustainable synthesis of nanomaterials, and materials science.

E-mail: ruslan.mariychuk@unipo.sk,

<https://orcid.org/0000-0001-8464-4142>

Вплив гетеровалентного $P^{+5} \leftrightarrow Si^{+4}$ заміщення на мікротвердість монокристалів $Ag_{7+x}(P_{1-x}Si_x)S_6$

І.О. Шендер, А.І. Погодін, М.Й. Філеп, Т.О. Малаховська, О.П. Кохан, Л.М. Сусліков, В.С. Біланіч, Р. Марійчук

Анотація. У даній роботі наведено результати дослідження мікротвердості монокристалів твердих розчинів $Ag_{7+x}(P_{1-x}Si_x)S_6$ ($x = 0, 0.1, 0.25, 0.5, 0.75, 1$). Досліджено вплив складу x на залежність мікротвердості (H) від прикладеного навантаження. Дослідження проводили в широкому діапазоні навантажень $0,05 \dots 2$ Н. Установлено, що збільшення навантаження на індентор приводить до монотонного нелінійного зменшення значень мікротвердості у всіх досліджуваних зразках. Це свідчить про «нормальний» розмірний ефект індентування. Спостережувані розмірні ефекти індентування у монокристалах $Ag_{7+x}(P_{1-x}Si_x)S_6$ описано в рамках моделі геометрично необхідних дислокацій. Визначено відповідні параметри моделі геометрично необхідних дислокацій. Обговорено вплив іонних радіусів та електронегативності структуроутворюючих елементів твердих розчинів $Ag_{7+x}(P_{1-x}Si_x)S_6$.

Ключові слова: аргіродити, монокристали, мікротвердість, гетеровалентне заміщення.